AGU PUBLICATIONS

JGR

Journal of Geophysical Research: Space Physics

RESEARCH ARTICLE
10.1002/2016JA023266

Key Points:
- Electric field antennas can be used to detect dust impacts on spacecraft
- The sensitivity of a dipole antenna to an impact on an antenna is similar to that of a monopole antenna to an impact on the spacecraft
- For Cassini/RPWS, dipole mode primarily detects impacts on the antenna elements

Correspondence to:
S.-Y. Ye,
shengyi-ye@uiowa.edu

Citation:
Ye, S.-Y., W. S. Kurth, G. B. Hospodarsky, T. F. Averkamp, and D. A. Gurnett (2016), Dust detection in space using the monopole and dipole electric field antennas, *J. Geophys. Res. Space Physics*, *121*, 11,964–11,972, doi:10.1002/2016JA023266.

Received 1 AUG 2016
Accepted 30 NOV 2016
Accepted article online 8 DEC 2016
Published online 22 DEC 2016

Dust detection in space using the monopole and dipole electric field antennas

S.-Y. Ye[1], W. S. Kurth[1], G. B. Hospodarsky[1], T. F. Averkamp[1], and D. A. Gurnett[1]

[1]Department of Physics and Astronomy, University of Iowa, Iowa City, Iowa, USA

Abstract During the grand finale of the Cassini mission, the Radio and Plasma Wave Science instrument will be used to assess the risk involved in exposing the instruments to the dusty environment around the F and D rings. More specifically, the slope of the size distribution and the dust density will be determined based on the signals induced on the electric antennas by dust impacts. To reduce the uncertainties in the generation mechanism of the dust impact signals and the resulting dust properties based on the interpretation of data, we designed and carried out experiments in late 2015, when we switched antenna mode from monopole to dipole at the ring plane crossings. Comparison of the data collected with these two antenna setups provides valuable hints on how the dust impact signals are generated in each antenna mode.

1. Introduction

The dust detection using electric field antennas began with incidental observations by the wave instruments onboard early missions like Voyager [*Aubier et al.*, 1983; *Gurnett et al.*, 1983]. Till today, the physics of the impact process, the generation of the impact signals, and the effect of the plasma environment on the impact signals are still not fully understood, which results in uncertainties in the dust properties derived from observations [*Ye et al.*, 2014]. More recent missions like Cassini and some planned missions are equipped with more sophisticated wave instruments which can be used to map out the previously unexplored dust environments. For example, Cassini is going to flyby between the D ring and Saturn during its grand finale. This demands a thorough understanding of the generation mechanism of the impact signals induced on the electric antennas by dust impacts.

The impact charge yield has been measured by recent laboratory experiments where iron projectiles are accelerated to tens of km/s before impacting on targets of common spacecraft surface materials in a vacuum chamber [*Collette et al.*, 2014]. The response of a simulated spacecraft and monopole antenna to dust impacts has also been studied with the same accelerator facility [*Collette et al.*, 2015]. However, no known dipole antenna experiment has been carried out so far. It has been noted that the dust impact signals observed by dipole electric antennas are significantly lower than those observed by monopole antennas [*Tsintikidis et al.*, 1994; *Meyer-Vernet et al.*, 2014], and the difference has been attributed to low sensitivity of dipole antennas to impacts on the spacecraft, yielding smaller pulses for the more numerous events.

In this paper, we report Cassini Radio and Plasma Waves Science (RPWS) instrument data collected during the ring plane crossings in late 2015 and early 2016, when experiments were designed to clarify the generation mechanism of dust impact signals on the monopole and dipole electric antennas. We analyze the data collected during these ring plane crossings and discuss the factors that might account for the observed differences in the monopole and dipole dust impact signals.

2. Instrument Description

The Cassini Radio and Plasma Wave Science (RPWS) instrument measures oscillating electric fields over the frequency range 1 Hz to 16 MHz and magnetic fields in the range 1 Hz to 12 kHz [*Gurnett et al.*, 2004]. The instrument uses three nearly orthogonal electric field antennas (Eu, Ev, and Ew, 10 m long each) and three orthogonal magnetic search coil antennas, providing a direction-finding capability. The Eu and Ev antennas are often used together as a dipole antenna and Ew as a monopole antenna [*Gurnett*, 1998].

The RPWS instrument has five receiver systems, only one of which is involved in this study, the high-resolution wideband receiver (WBR) that covers two frequency bands, 60 Hz to 10.5 kHz and 800 Hz to 75 kHz. The WBR records waveform snapshots of voltages measured on the RPWS antennas (either monopole

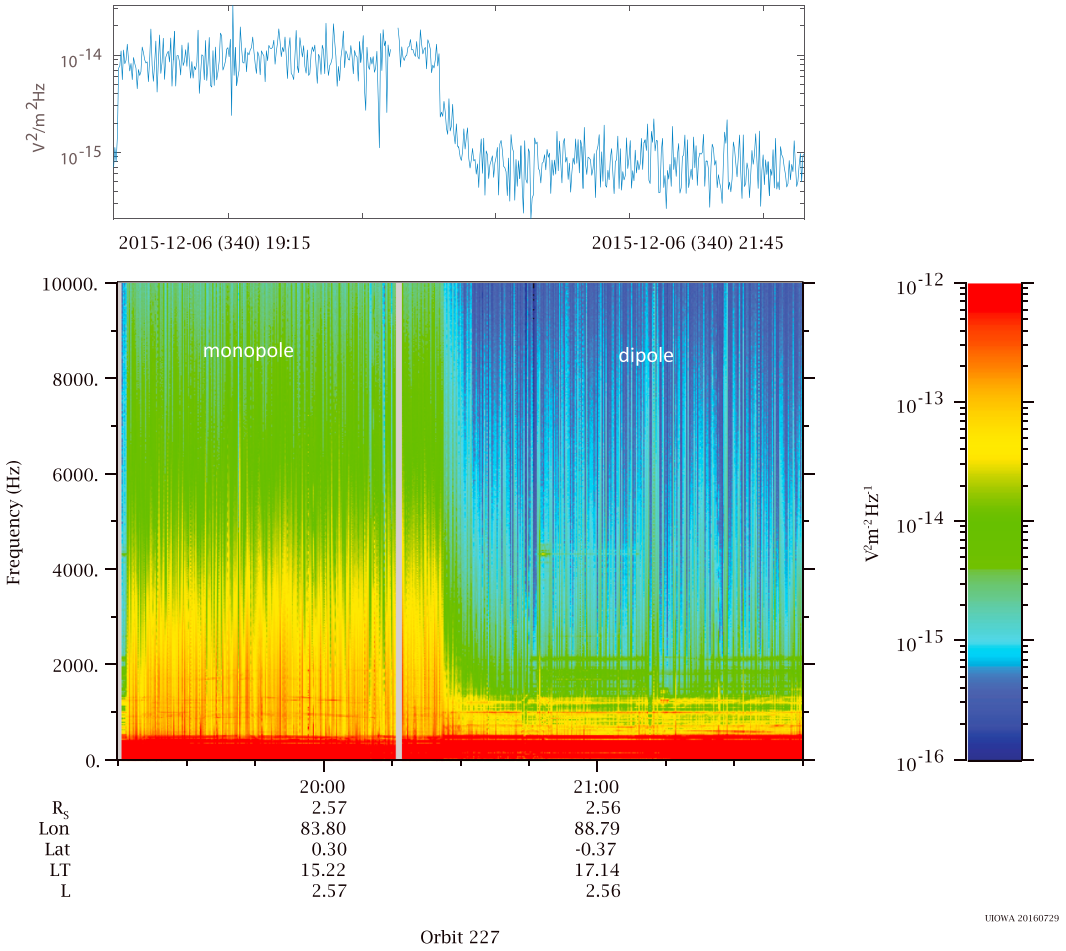

Figure 1. RPWS wave power spectrogram covers a 2 h period around a ring plane crossing on DOY 340, 2015. (top) The electric field wave power at 6 kHz. At 20:26, the antenna used was switched from monopole to dipole. Note that the wave power decreased by ~10 dB at the crossing.

or dipole), which can be Fourier transformed to provide high-resolution spectra of low-frequency radio and plasma waves as well as dust impact signatures. Due to the limited dynamic range afforded by the 8 bit analog-to-digital converter used, the gain of the receiver is automatically selected from 0 to 70 dB in 10 dB steps to accommodate signals induced by the waves and dust impacts.

3. Ring Plane Crossing Observations

During the Voyager flybys of Saturn, the Plasma Wave Subsystem (PWS) and Planetary Radio Astronomy (PRA) instruments both detected dust impact signals. By comparing the wave power spectra measured by the two instruments, *Tsintikidis et al.* [1994] concluded that the PRA instrument is 30–50 times more sensitive to dust impacts than PWS. They proposed that the difference could be due to the lower charge-antenna coupling efficiency and the common mode rejection of the dipole mode. The common mode rejection basically means that the common signal observed by the two antenna elements of the dipole mode will be subtracted out by the differential amplifier. So a voltage pulse on the spacecraft body (induced by dust impacts) will not be observed in the dipole mode. *Meyer-Vernet et al.* [2009, 2014] compared the dust signals observed in monopole and dipole modes on Cassini and concluded that the monopole antennas generally detect much greater signals than dipole antenna, because most of the impact charges are recollected by the spacecraft body. However, all these studies compared the spectra not the waveforms captured by the two antenna modes.

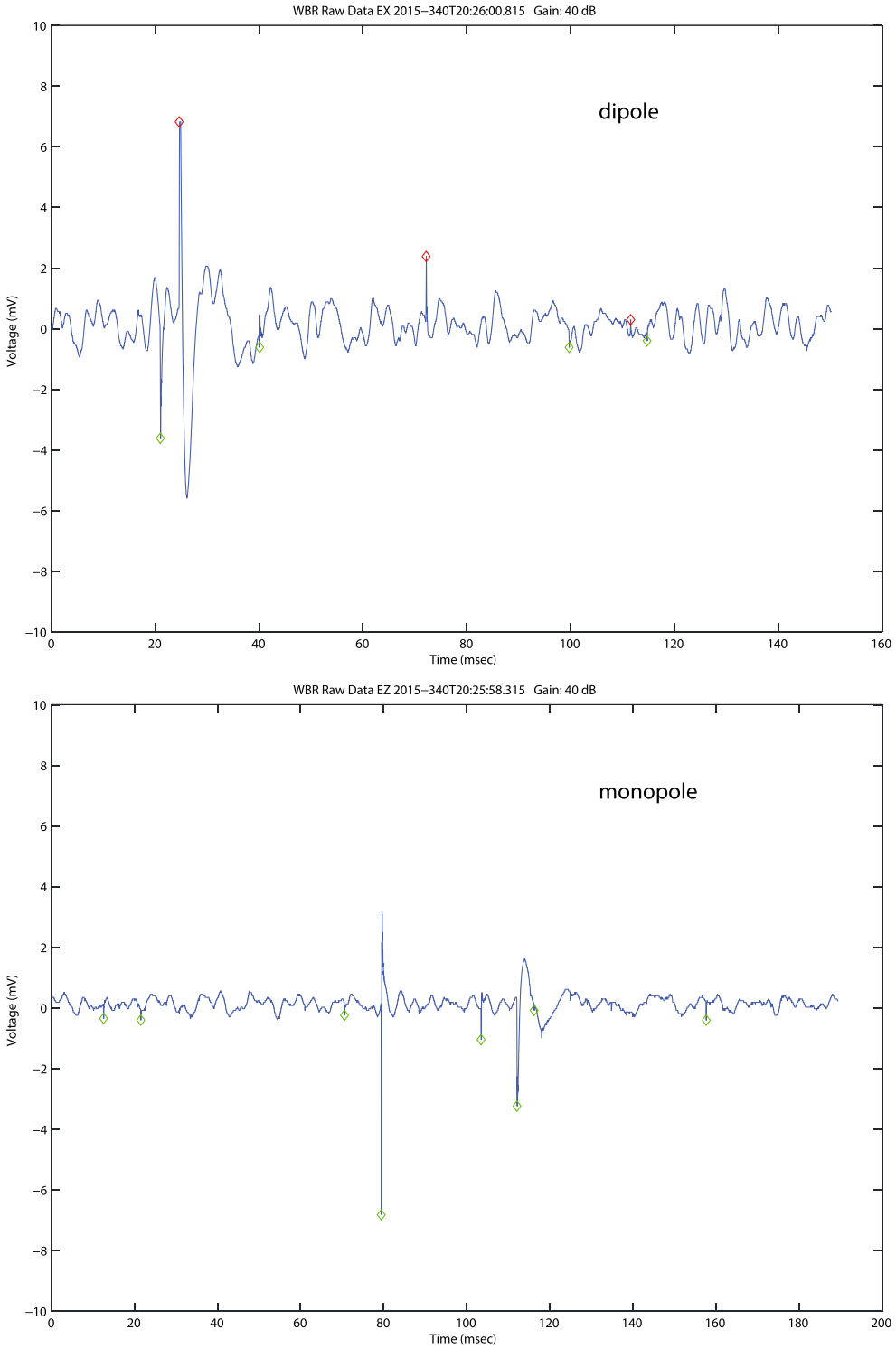

Figure 2. Comparison of waveforms of dust impacts observed by dipole and monopole antennas. The two snapshots are taken right before and after the antenna switch. Note that the impact voltage jumps induced on the two antennas are comparable.

Ye et al. [2014] compared the waveforms of dust impacts observed by the monopole and dipole antennas of the Cassini RPWS and showed that the dust signals detected by the monopole antenna were more than an order of magnitude stronger than those detected by the dipole antenna. However, the two sets of data compared are widely separated in both space and time. The monopole data were collected near the G ring

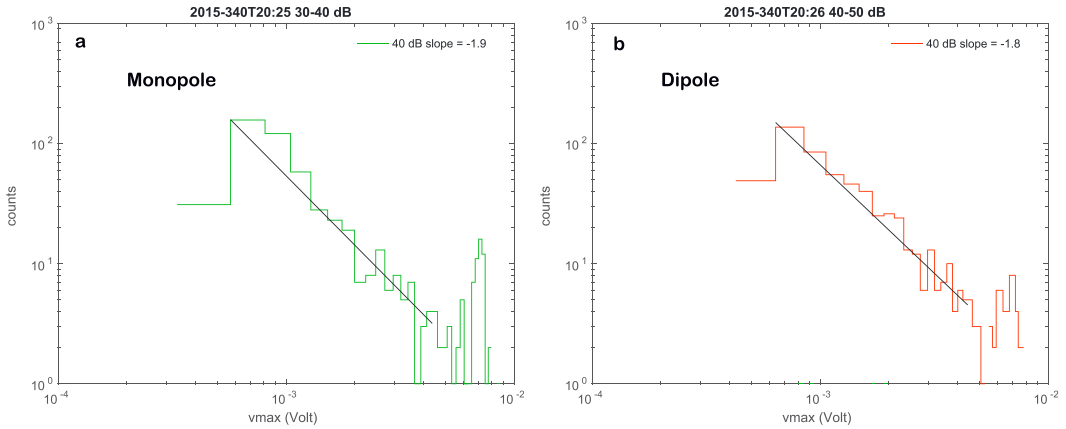

Figure 3. Histograms showing the impact voltage jump sizes observed on the dipole and monopole antennas. The two histograms contain data for 1 min each (same sampling rate and duty cycle) before and after the antenna switch. The peaks at around 7 mV in both histograms are due to clipped voltage pulses. The power law distribution would have continued to larger voltages if the dynamic range is larger.

on day of year (DOY) 248, 2005, and the dipole data were collected in the core of the E ring on DOY 159, 2005. The difference in signal amplitudes could be largely due to the difference in particle sizes in these two locations. To compare the response of monopole and dipole antennas to dust impacts, we need simultaneous waveform observations in both modes. But the WBR cannot be connected to both the dipole and monopole antennas at the same time. So instead, we switch the antenna mode from monopole to dipole at a location of high dust density, e.g., the ring plane. This way we can indirectly compare the response of these two antenna modes to dust impacts, assuming that the dust density and size distribution do not change across the ring plane.

Figure 1 shows an RPWS wave power spectrogram, which covers a 2 h period around a ring plane crossing on DOY 340, 2015. The antenna mode was switched from monopole to dipole at the ring plane at 20:26. Note that the wave power decreases by ~10 dB at the crossing, which is consistent with the difference between the monopole and dipole antenna observations shown by previous studies [e.g., *Tsintikidis et al*., 1994; *Meyer-Vernet et al*., 2014]. As modeled by *Meyer-Vernet et al*. [2009], the spectral power is proportional to the product of impact rate and average squared voltage pulse amplitude. So the difference in spectral power at the antenna switch could be due to either lower impact rate or smaller average voltage pulse size, or both. We need to compare the waveforms to tell which factors contribute the most to the power decrease.

In Figure 2, we compare waveforms of dust impacts observed by the dipole and monopole antennas. The two snapshots are taken right before and after the antenna switch. Note that the impact voltage jumps induced on the two antennas are comparable. The monopole antenna detects more dust impacts in a snapshot and polarities of the pulses are mostly negative. Figure 3 shows histograms of the impact voltage pulse sizes observed on the dipole and monopole antennas. The two histograms contain data for 1 min each (same sampling rate and duty cycle) before and after the antenna switch. The comparison shows that the ranges of voltage pulse sizes observed in the two antenna modes are comparable if not equal. In fact, the voltage pulses measured by dipole antennas are comparable to and sometimes even stronger than those measured by monopole antennas. Therefore, the higher spectral power observed by monopole antennas might be a result of higher impact rates. This was pointed out by *Meyer-Vernet et al*. [2014] as a possible explanation for the smaller power spectrum observed by dipole antenna, which has a smaller cross-sectional area than the spacecraft body.

Figure 4 shows an RPWS wave power spectrogram covering a 1 h period around a ring plane crossing on DOY 001, 2016, where the antenna was switched from monopole to dipole at around 10:30. Note the wave power decrease (more than 10 dB) at the crossing indicated by the white arrow. Assuming continuity of dust density at the ring plane, the decrease in wave power could be due to either lower sensitivity (smaller dust impact signal measured) or smaller effective impact area (fewer dust impacts detected) of the dipole mode. Examination of the waveforms before and after the antenna switch confirms that the voltage pulses detected by the two antenna modes are comparable, similar to the comparisons shown in Figures 2 and 3.

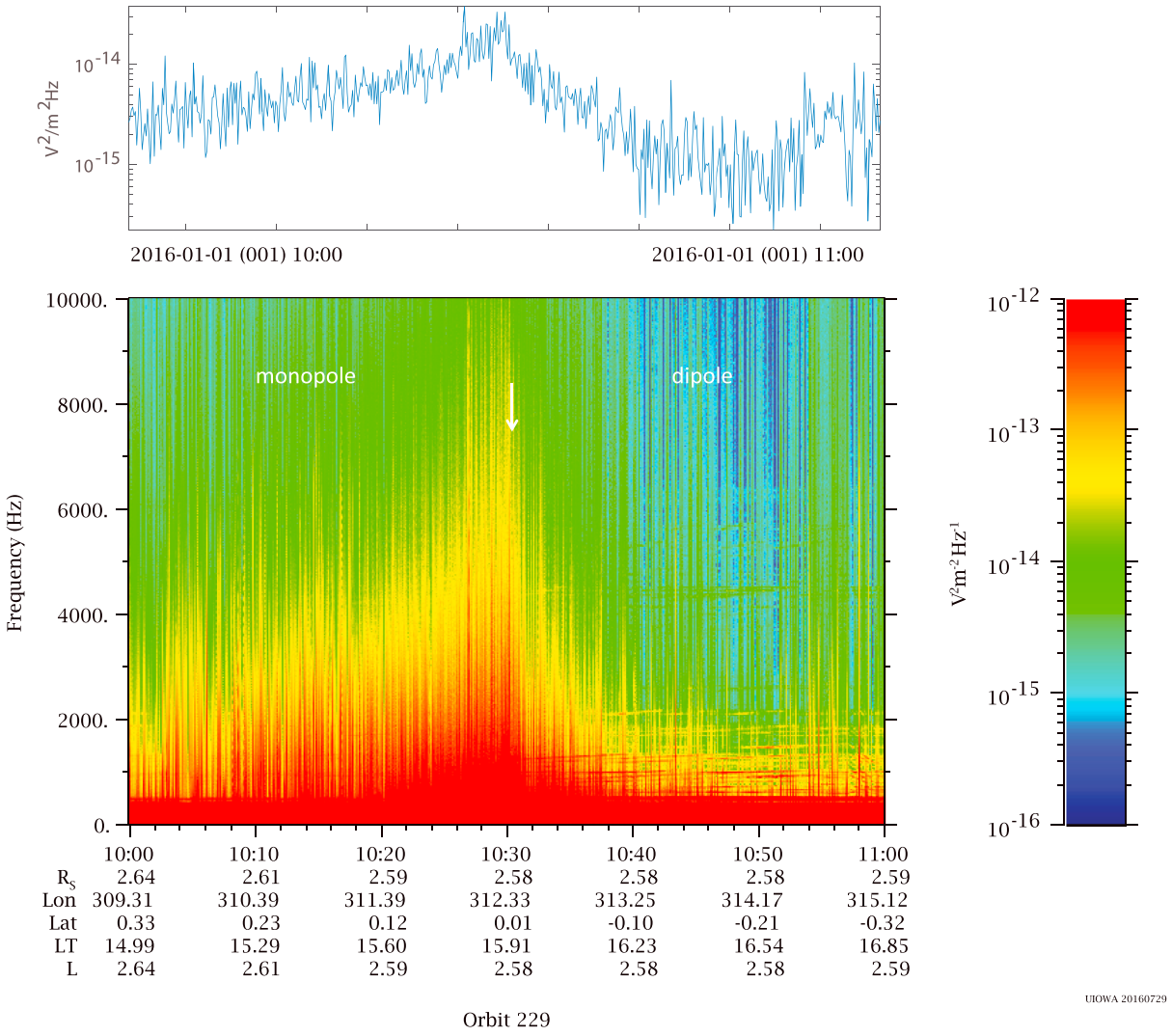

Figure 4. RPWS wave power spectrogram covers a 1 h period around a ring plane crossing on DOY 001, 2016. (top) The electric field wave power at 9 kHz. At 10:30, the antenna used was switched from monopole to dipole. Note the wave power decreased at the crossing indicated by the white arrow.

Figure 5a shows the dust impact rates (separated by the polarity of the voltage jumps) measured by the RPWS wideband receiver during the same ring plane crossing as shown in Figure 4 on DOY 001, 2016. It is noticed that the counting rates of negative voltage jumps (blue) are 5–6 times larger than the counting rates of positive voltage jumps (red) before the antenna switch at around 10:30. However, the counting rates of positive impacts before the switch are similar to the counting rates of the positive and negative impacts after the antenna switch. Figure 5b shows the ratio of positive to negative impact rates (plus signs) with moving averages (20 s window) overplotted (teal). It is clear that this ratio jumps from 0.1 to 0.2 to around 1 at the antenna switch. Figure 5c shows the angles between the ram direction and the electric antenna elements Eu (red), Ev (blue), and Ew (green). These angles are subject to change as the attitude of the spacecraft changes. As a result, the effective areas of the three electric antenna elements also change with the attitude of Cassini. As discussed by *Ye et al.* [2014], the difference between the positive and negative impact rates measured by the monopole antenna indicates that the negative voltage pulses are due to impacts on the spacecraft body (6.7 m tall, 4 m wide, and ~12 m^2 effective area for the High Gain Antenna), whereas the positive ones are due to impacts on the Ew antenna element (10 m long, 2.86 cm diameter, and ~0.2 m^2 effective impact area). The impact rates measured by the dipole antenna (both positive and negative) are comparable to the positive impact rates measured by the monopole antenna (as shown in Figure 5a), indicating that these voltage pulses are all due to impacts on the antenna elements (Eu and Ev for positive/negative signals measured by the dipole antenna). Note that the sign of the floating potential of the spacecraft and antennas plays

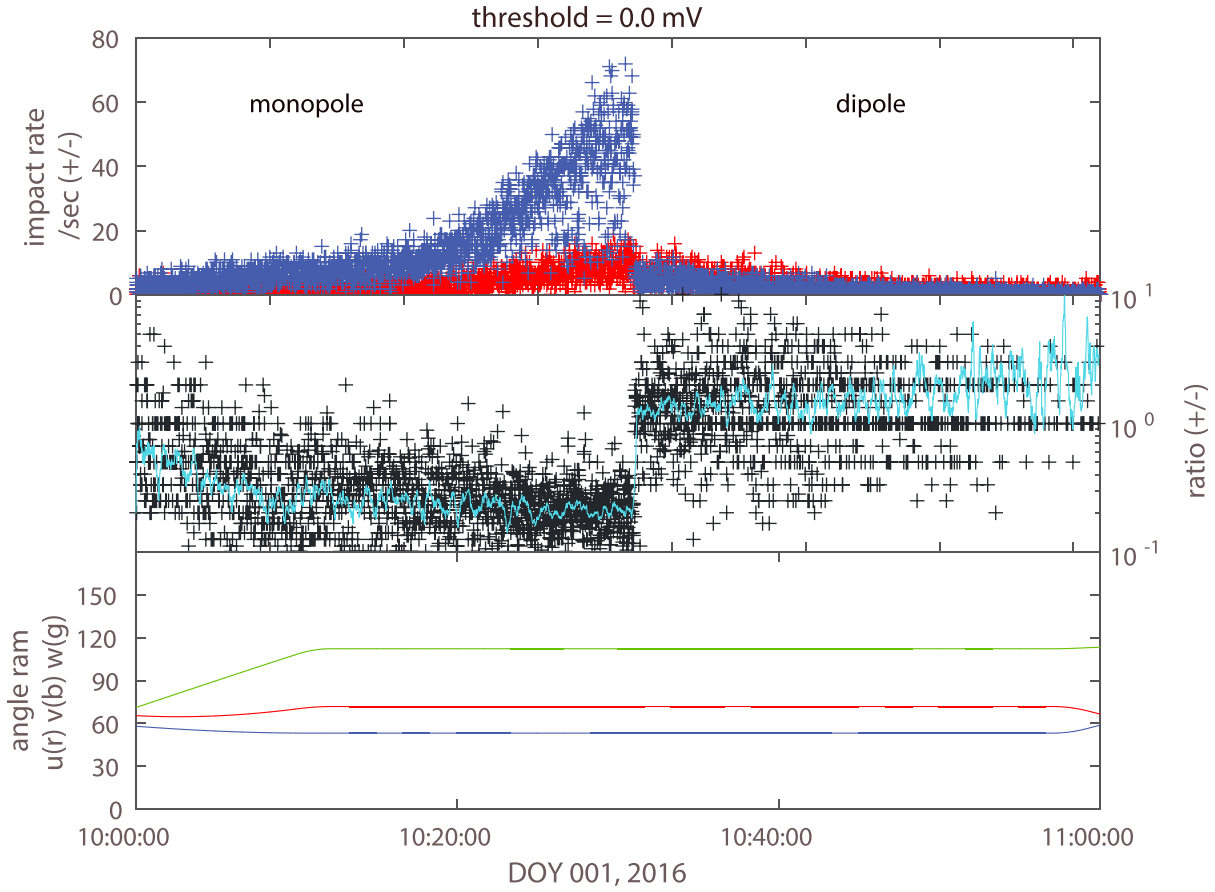

Figure 5. Statistics of dust impacts observed during the ring plane crossing on DOY 001, 2016. (a) Counting rates of positive (red) and negative (blue) voltage jumps induced by dust impacts. (b) Positive to negative impact rate ratio (plus signs) with the moving averages over plotted (teal). (c) Angles between the ram direction and the electric antenna elements Eu (red), Ev (blue), and Ew (green).

an important role, since it determines whether the surfaces will recollect electrons or ions, whose motional time scales are very different. In the cases studied here, the spacecraft potential was negative [*Wahlund et al*., 2005; *Sittler et al*., 2006]. The physics will be different when the spacecraft potential is positive (in dilute plasmas or at smaller heliocentric distances).

Figure 6 shows the statistics of dust impacts observed during the E21 flyby on DOY 301, 2015. During the whole period shown, dipole antenna was used (the antenna mode was switched from monopole to dipole earlier during the ring plane crossing, which is not shown). The dust impacts are separated by the polarity of the voltage jumps when we calculate the impact rates. Figure 6a shows that the positive and negative impact rates detected by the dipole antenna are generally comparable. The impact rates peak at the time of the Enceladus plume crossing, which is expected. Figure 6b shows the polarity ratio is mostly around 1 except two times when the spacecraft was rotating, as shown by the varying ram-antenna angles in Figure 6c.

Figure 7 compares the polarity ratio of dust impacts detected by the dipole antenna during the E21 flyby with the ratio of the projected antenna areas between two elements the dipole antenna Eu and Ev. The projected antenna areas are calculated based on the ram-antenna angles shown in Figure 6c. It is shown that the polarity ratio of the dust impacts measured by the dipole antenna closely matches the ratio of the projected areas of the dipole antenna elements. The coincident sharp rises of the polarity and projected area ratio to around 10 are caused by the spacecraft rotation, when the Ev element is almost parallel to the ram direction, which greatly reduces the effective impact area and the number of negative impacts. The correspondence between the polarity ratio and the antenna projected area ratio indicates that the dust impact signals observed by the dipole antenna are primarily due to dust impacts on the electric antenna elements, namely, Eu and Ev.

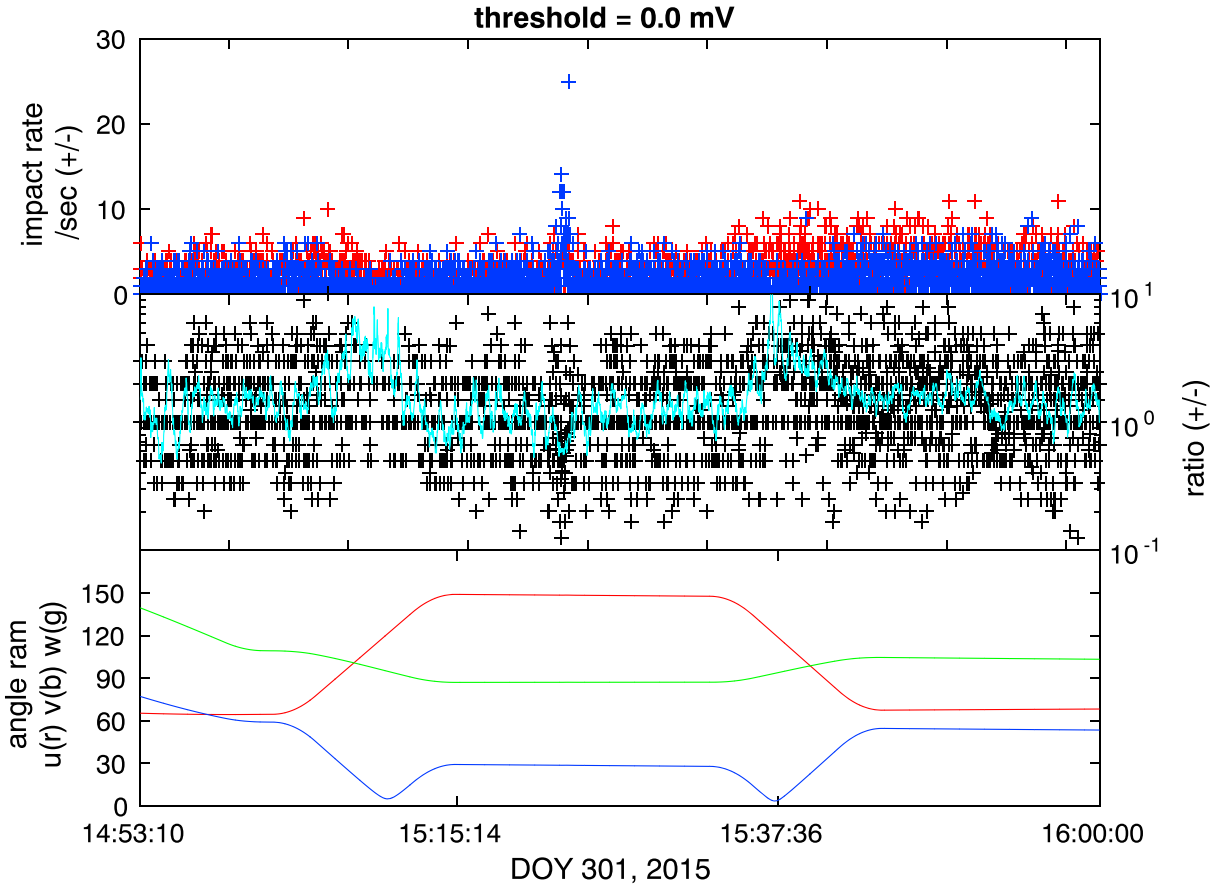

Figure 6. Statistics of dust impacts observed by the dipole antenna during the E21 flyby on DOY 301, 2015. (a) Counting rates of positive (red) and negative (blue) voltage jumps induced by dust impacts. (b) Positive to negative impact rate ratio (plus signs) with the moving averages over plotted (teal). (c) Angles between the ram direction and the electric antenna elements Eu (red), Ev (blue), and Ew (green).

4. Discussion

Hypervelocity impacts of dust particles on spacecraft generate expanding plasma clouds that induce transient voltage signals detectable by electric field antennas of radio and plasma wave instruments, e.g., Voyager PWS [*Scarf et al.*, 1982] and PRA [*Meyer-Vernet et al.*, 1996], Cassini RPWS [*Gurnett et al.*, 2005], STEREO WAVES [*Zaslavsky et al.*, 2012], Wind WAVES [*Malaspina et al.*, 2014, *Kellogg et al.*, 2016] and MAVEN LPW [*Andersson et al.*, 2015]. The generation mechanism of the dust impact signals picked up by the electric field antennas has been proposed and discussed by many previous studies [*Gurnett et al.*, 1983; *Meyer-Vernet*, 1985; *Meyer-Vernet et al.*, 1986; *Gurnett et al.*, 1987, 1991; *Oberc*, 1996; *Tsurutani et al.*, 2004; *Kurth et al.*, 2006; *Wang et al.*, 2006; *Schippers et al.*, 2014; *Ye et al.*, 2014]. Generally, all scenarios discussed involve vaporization of the dust particle and part of the target material due to the energy released during the hypervelocity impact. The resulting plasma cloud then couple to the electric antennas/spacecraft body by either direct charge collection or drawing image charges on them.

Collette et al. [2015] carried out laboratory experiments modeling the electric field antenna pickup of signals induced by dust impact on a spacecraft body. It was shown that the charge recollection by the target impacted on plays a major role in the generation of the signals, although a small signal preceding the main voltage spike called prespike was identified and proposed to be induced by the ambipolar electric field generated by the charge separation between the electrons and ions after impact. By analyzing Cassini RPWS data, it was also found that the choice of antenna mode (either monopole or dipole mode) turns out to have a significant impact on the efficiency of charge collection and the resulting power spectral density [*Meyer-Vernet et al.*, 2009, 2014]. However, due to the lack of direct comparison of waveforms observed by the dipole and monopole antennas, they could not differentiate between lower impact rate

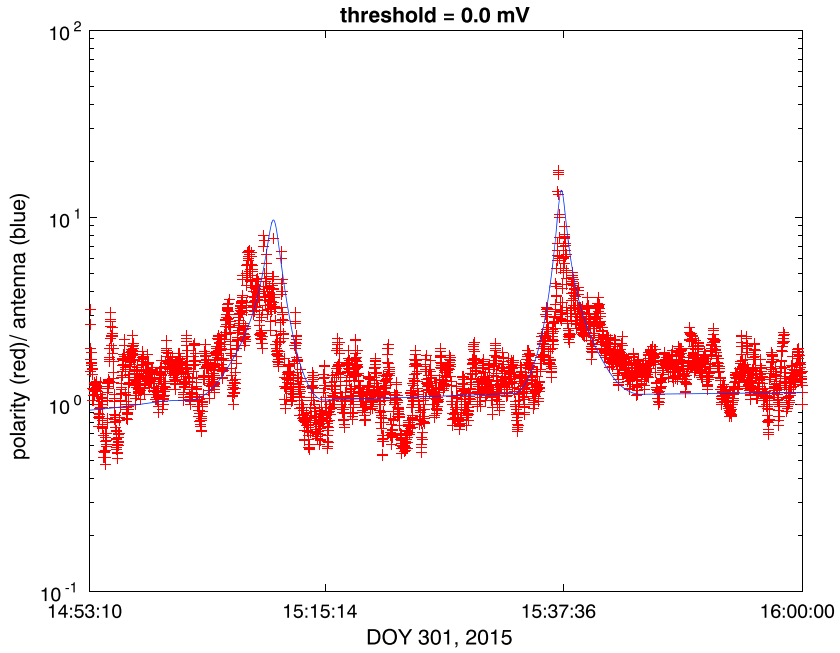

Figure 7. Polarity ratios of dust impacts (red plus signs) observed by the dipole antenna during the E21 flyby on DOY 301, 2015. The blue line is the ratio of the Eu and Ev antenna projected area as seen from the ram direction, which varies due to the spacecraft rotation. Note that the polarity ratio seems to change with the projected antenna area ratio.

and smaller individual signals as the cause for the lower power spectral density observed on the dipole antenna. So they interpreted the lower signal level detected by the dipole antenna as a result of lower sensitivity of the antenna to the impact plasma cloud due to the long distance between the antenna elements and the impact site (spacecraft body).

This study compared the dust impact-induced waveforms observed by the dipole and monopole antennas for the first time. Although Cassini RPWS wideband receiver cannot take measurements on the dipole and monopole antennas at the same time, we chose to switch the antenna at the equator during the ring plane crossings. Assuming that the vertical density profile is symmetric with respect to the equator, we were able to make an indirect comparison of the responses of the dipole and monopole antenna to the dust impacts. The results showed that the dipole antenna is at least as sensitive to dust impacts as the monopole antenna. Instead, we found that the impact rate observed by the monopole antenna is significantly higher than that of the dipole antenna. When we separate the impact signals by polarity, the counting rate of the positive voltage pulses observed on the monopole antenna is similar to counting rates of the positive and negative voltage pulses observed on the dipole antenna, and they are significantly smaller than the counting rate of the negative voltage pulses observed on the monopole antenna. These impact rate ratios are consistent with effective impact area ratios of the different elements of the antennas. More specifically, the three electric antenna booms have roughly the same impact area, while the spacecraft body (the other element of the monopole antenna) has the largest effective impact area. So the stronger dust impact signal (power spectral density) observed by the monopole antenna is actually due to the higher impact rates, thanks to the larger effective impact area of the spacecraft body.

5. Summary

Based on recent RPWS wideband receiver observations in late 2015 and early 2016, when the antenna mode was switched from monopole to dipole at the ring plane crossings, we compared the data collected with these two antenna setups, which provided valuable hints on how the dust impact signals are generated in each antenna mode. The comparison showed that the wave power spectral density observed by the monopole antenna is ~10 dB higher than that observed by the dipole antenna. This does not necessarily mean that the monopole antenna is more sensitive to dust impacts, because when we directly compared the

waveforms observed by these two antennas, the size of voltage jumps induced by the dust impacts are comparable. Comparison of the impact rates showed that the monopole antenna detects ~10 times more dust impacts than the dipole antenna. This difference in impact rates is roughly in line with the difference in the effective areas of the spacecraft body and the dipole electric antenna. Detailed analysis of the dust impacts detected by the dipole antenna showed that the polarity ratio of the impacts is consistent with the projected area ratio of the dipole antenna elements (Eu and Ev), providing strong evidence that the dipole mode detects primarily impacts on the antenna booms. So RPWS can actually detect dust impacts on at least four different sensors, namely, three electric antennas (Eu, Ev, and Ew) and the spacecraft body. These new understandings of the generation process of the dust impact signals observed by electric field antennas will greatly reduce the uncertainty associated with the interpretation of future dust impacts data collected by wave instruments, most importantly during the Cassini proximal orbits.

Acknowledgments
This research was supported by NASA through contract 1415150 with the Jet Propulsion Laboratory. The data used in this study are available through the Planetary Data System or from the authors.

References

Andersson, L., et al. (2015), Dust observations at orbital altitudes surrounding Mars, *Science*, *350*(6261, p.aad0398).
Aubier, M. G., N. Meyer-Vernet, and B. M. Pedersen (1983), Shot noise from grain and particle impacts in Saturn's ring plane, *Geophys. Res. Lett.*, *10*, 5–8, doi:10.1029/GL010i001p00005.
Collette, A., E. Grün, D. Malaspina, and Z. Sternovsky (2014), Micrometeoroid impact charge yield for common spacecraft materials, *J. Geophys. Res. Space Physics*, *119*, 6019–6026, doi:10.1002/2014JA020042.
Collette, A., G. Meyer, D. Malaspina, and Z. Sternovsky (2015), Laboratory investigation of antenna signals from dust impacts on spacecraft, *J. Geophys. Res. Space Physics*, *120*, 5298–5305, doi:10.1002/2015JA021198.
Gurnett, D. A. (1998), Principles of space plasma wave instrument design, in *Measurement Techniques for Space Plasmas*, *AGU Monogr.*, vol. 103, edited by R. Pfaff, J. Borovsky, and D. Young, pp. 121–136, AGU, Washington, D. C.
Gurnett, D. A., E. Grün, D. Gallagher, W. S. Kurth, and F. L. Scarf (1983), Micron-sized particles detected near Saturn by the Voyager plasma wave instrument, *Icarus*, *53*, 236–254, doi:10.1016/0019-1035(83)90145-8.
Gurnett, D. A., W. S. Kurth, F. L. Scarf, J. A. Burns, J. N. Cuzzi, and E. Grün (1987), Micron-sized particle impacts detected near Uranus by the Voyager 2 plasma wave instrument, *J. Geophys. Res.*, *92*, 14,959–14,968, doi:10.1029/JA092iA13p14959.
Gurnett, D. A., W. S. Kurth, L. J. Granroth, S. C. Allendorf, and R. L. Poynter (1991), Micron-sized particles detected near Neptune by the Voyager 2 plasma wave instrument, *J. Geophys. Res.*, *96*, 19,177–19,186, doi:10.1029/91JA01270.
Gurnett, D. A., et al. (2004), The Cassini radio and plasma wave science investigation, *Space Sci. Rev.*, *114*, 395–463.
Gurnett, D. A., et al. (2005), Radio and plasma wave observations at Saturn from Cassini's approach and first orbit, *Science*, *307*(5713), 1255–1259, doi:10.1126/science.1105356.
Kellogg, P. J., K. Goetz, and S. J. Monson (2016), Dust impact signals on the Wind spacecraft, *J. Geophys. Res. Space Physics*, *121*, 966–991, doi:10.1002/2015JA021124.
Kurth, W. S., T. F. Averkamp, D. A. Gurnett, and Z. Wang (2006), Cassini RPWS observations of dust in Saturn's E ring, *Planet. Space Sci.*, *54*, 988–998, doi:10.1016/j.pss.2006.05.011.
Malaspina, D. M., M. Horányi, A. Zaslavsky, K. Goetz, L. B. Wilson, and K. Kersten (2014), Interplanetary and interstellar dust observed by the Wind/WAVES electric field instrument, *Geophys. Res. Lett.*, *41*, 266–272, doi:10.1002/2013GL058786.
Meyer-Vernet, N. (1985), Comet Giacobini-Zinner diagnosis from radio measurements, *Adv. Space Res.*, *5*, 37–46, doi:10.1016/0273-1177(85)90065-1.
Meyer-Vernet, N., P. Couturier, S. Hoang, C. Perche, J. L. Steinberg, J. Fainberg, and C. Meetre (1986), Plasma diagnosis from thermal noise and limits on dust flux or mass in comet Giacobini-Zinner, *Science*, *232*(4748), 370–374, doi:10.1126/science.232.4748.370.
Meyer-Vernet, N., A. Lecacheux, and B. M. Pedersen (1996), Constraints on Saturn's E ring from the Voyager 1 radio astronomy instrument, *Icarus*, *123*, 113–129, doi:10.1006/icar.1996.0145.
Meyer-Vernet, N., A. Lecacheux, M. L. Kaiser, and D. A. Gurnett (2009), Detecting nanoparticles at the radio frequencies: Jovian dust stream impacts on Cassini/RPWS, *Geophys. Res. Lett.*, *36*, L03103, doi:10.1029/2008GL036752.
Meyer-Vernet, N., M. Moncuquet, K. Issautier, and A. Lecacheux (2014), The importance of monopole antennas for dust observations: Why Wind/WAVES does not detect nanodust, *Geophys. Res. Lett.*, *41*, 2716–2720, doi:10.1002/2014GL059988.
Oberc, P. (1996), Electric antenna as a dust detector, *Adv. Space Res.*, *17*, 105–110, doi:10.1016/0273-1177(95)00766-8.
Scarf F. L., D. A. Gurnett, W. S. Kurth, and R. L. Poynter (1982), Voyager 2 Plasma Wave Observations at Saturn, *Science*, *215*(4532), 587–594.
Schippers, P., N. Meyer-Vernet, A. Lecacheux, W. S. Kurth, D. G. Mitchell, and N. Andre (2014), Nanodust detection near 1 AU from spectral analysis of Cassini/Radio and Plasma Wave Science data, *Geophys. Res. Lett.*, *41*, 5382–5388, doi:10.1002/2014GL060566.
Sittler, E. C., et al. (2006), Cassini observations of Saturn's inner plasmasphere: Saturn orbit insertion results, *Planet. Space Sci.*, *54*(12), 1197–1210, doi:10.1016/j.pss.2006.05.038.
Tsintikidis, D., D. A. Gurnett, L. J. Granroth, S. C. Allendorf, and W. S. Kurth (1994), A revised analysis of micron-sized particle detected near Saturn by the Voyager 2 plasma wave instrument, *J. Geophys. Res.*, *99*, 2261–2270, doi:10.1029/93JA02906.
Tsurutani, B. T., D. R. Clay, L. D. Zhang, B. Dasgupta, D. Brinza, M. Henry, J. K. Arballo, S. Moses, and A. Mendis (2004), Plasma clouds associated with Comet P Borrelly dust impacts, *Icarus*, *167*(1), 89–99, doi:10.1016/j.icarus.2003.08.021.
Wahlund, J. E., et al. (2005), The inner magnetosphere of Saturn: Cassini RPWS cold plasma results from the first encounter, *Geophys. Res. Lett.*, *32*, L20S09, doi:10.1029/2005GL022699.
Wang, Z., D. A. Gurnett, T. F. Averkamp, A. M. Persoon, and W. S. Kurth (2006), Characteristics of dust particles detected near Saturn's ring plane, *Planet. Space Sci.*, *54*, 957–966, doi:10.1016/j.pss.2006.05.015.
Ye, S. -Y., D. A. Gurnett, W. S. Kurth, T. F. Averkamp, S. Kempf, H. W. Hsu, R. Srama, and E. Gruen (2014), Properties of dust particles near Saturn inferred from voltage pulses induced by dust impacts on Cassini spacecraft, *J. Geophys. Res. Space Physics*, *119*, 6294–6312, doi:10.1002/2014JA020024.
Zaslavsky, A., et al. (2012), Interplanetary dust detection by radio antennas: Mass calibration and fluxes measured by STEREO/WAVES, *J. Geophys. Res.*, *117*, A05102, doi:10.1029/2011JA017480.